Superconducting phases in $(NH_3)_y M_x FeSe_{1-z}Te_z$ (M = Li, Na, and Ca)

Yusuke Sakai,[1] Lu Zheng,[1] Masanari Izumi,[1] Kazuya Teranishi,[1] Ritsuko Eguchi,[1] Hidenori Goto,[1] Taiki Onji,[2]
Shingo Araki,[2] Tatsuo C. Kobayashi,[2,3] and Yoshihiro Kubozono[1,3,*]

[1]*Research Laboratory for Surface Science, Okayama University, Okayama 700-8530, Japan*
[2]*Department of Physics, Okayama University, Okayama 700-8530, Japan*
[3]*Research Center of New Functional Materials for Energy Production, Storage and Transport, Okayama University,
Okayama 700-8530, Japan*

Superconducting phases of $(NH_3)_y M_x FeSe_{1-z}Te_z$ have been synthesized by the intercalation of metal atoms
(M: Li, Na, Ca) into FeSe and $FeSe_{0.5}Te_{0.5}$ using a low-temperature liquid NH_3 technique. The superconducting
transition temperature (T_c) is 31.5 K for Na-doped FeSe, and for Li-, Na-, and Ca-doped $FeSe_{0.5}Te_{0.5}$ it is 26, 22,
and 17 K, respectively. The 31.5 K superconducting is the superconducting phase in ammoniated Na-doped FeSe.
The T_c is lower than that (onset T_c = 46 K) of the superconducting phase reported previously. The reason why the T_c
of this phase is lower is discussed based on the structure. The pressure dependences of T_c in the $(NH_3)_y Na_{0.5}FeSe$
and $(NH_3)_y Na_{0.4}FeSe_{0.5}Te_{0.5}$ samples have been measured and a negative pressure dependence is observed;
i.e., a decrease in lattice constant c leads to a decrease in T_c, consistent with the behavior of $(NH_3)_y Cs_{0.4}FeSe$
reported previously by our group. Furthermore, the magnetic behavior of $(NH_3)_y Na_{0.4}FeSe_{0.5}Te_{0.5}$ has been fully
investigated at different applied magnetic fields (H) to determine the critical magnetic field. This is a successful
metal intercalation into $FeSe_{1-z}Te_z$ ($z \neq 0$) and an observation of superconductivity.

Metal-intercalated FeSe superconductors prepared using an
annealing technique [1,2] and a liquid NH_3 technique [3–6]
have been extensively studied because of their high super-
conducting transition temperatures (T_c). The $(NH_3)_y M_x FeSe$
materials synthesized using the liquid NH_3 technique contain
NH_3 molecules between the FeSe layers [3–6]. The expansion
of lattice constant c, i.e., the plane spacing between FeSe layers
owing to insertion of NH_3 molecules, produced higher T_c's
than those of materials without NH_3 [6]. The highest T_c is now
46 K for $(NH_3)_y Na_{0.5}FeSe$ in the $(NH_3)_y M_x FeSe$ materials
prepared using the liquid NH_3 technique [3]. To exceed
superconductivity of 46 K is currently the most important
research subject in this field. Very recently, we succeeded in
synthesizing an $(NH_3)_y Cs_{0.4}FeSe$ sample showing a T_c as high
as 33.6 K [6]. This study showed that the T_c increased with the
intercalation of ions with smaller ionic radius. Furthermore,
a correlation between lattice constant c and T_c was clearly
shown in the $(NH_3)_y M_x FeSe$ materials [6]. Thus, increasing
two dimensionality or Fermi-surface nesting is a key for raising
the T_c in these materials, as in HfNCl [7,8].

Recently, a phase of $(NH_3)_y K_x FeSe$ exhibiting a higher
T_c (=44 K) than that of a previous sample (T_c = 30 K)
was discovered [5], which suggested the presence of mul-
tiple superconducting phases even though the samples were
prepared with the same stoichiometric amounts of metal.
Actually, the two phases are isostructural but the c (=15.56 Å)
in the former phase is larger than that (=14.84 Å) in the
latter phase, suggesting that the increase in c produced the
higher-T_c phase [5]. This provides a motivation to search
for new superconducting phases in $(NH_3)_y M_x FeSe$, i.e., new
superconducting phases with T_c's higher than ~45 K may
be masked even in $(NH_3)_y Na_{0.5}FeSe$ and $(NH_3)_y Li_{0.5}FeSe$ [3]

exhibiting the T_c of ~45 K. Furthermore, it should be noted that
metal intercalation has never been achieved for $FeSe_{1-z}Te_z$
($z \neq 0$), regardless of the possibility that the T_c may increase
because the T_c of pure $FeSe_{1-z}Te_z$ ($0 \leqslant z \leqslant 0.8$) without
metal intercalation is higher than that of FeSe (T_c = 8 K)
[9,10]. Furthermore, the c of $FeSe_{1-z}Te_z$ ($0 \leqslant z \leqslant 0.8$) is
larger than that of FeSe and the c increases with an increase
in z [11]. Therefore, the metal intercalation into $FeSe_{1-z}Te_z$ is
very exciting and significant.

In the present study, we have searched for supercon-
ducting phases in $(NH_3)_y M_x FeSe_{1-z}Te_z$ (z = 0 and 0.5).
We have found a superconducting phase in $(NH_3)_y Na_x FeSe$
with a T_c^{onset} of 36 K, which is lower than the 46 K, in
the previous report [3], which demonstrates the presence
of multiple superconducting phases. The structures of two
superconducting phases (T_c^{onset} = 36 K and T_c^{onset} = 46 K)
in $(NH_3)_y Na_x FeSe$ were determined from the Le Bail fitting
of x-ray diffraction (XRD) patterns, in order to clarify the
origin of the different T_c. We succeeded in intercalating
Li, Na, and Ca metal atoms into β-$FeSe_{0.5}Te_{0.5}$ using the
liquid NH_3 technique, and these samples showed T_c's different
from the corresponding FeSe materials. Thus, we have found
alternative superconductors in the FeSeTe system. The crystal
structure of $(NH_3)_y Na_{0.4}FeSe_{0.5}Te_{0.5}$ is also determined from
the Le Bail fitting of the XRD pattern, and the lattice
constants are compared with two $(NH_3)_y Na_x FeSe$ phases.
The pressure dependences of T_c in $(NH_3)_y Na_{0.5}FeSe$ and
$(NH_3)_y Na_{0.4}FeSe_{0.5}Te_{0.5}$ have also been investigated and
compared with the $(NH_3)_y Cs_{0.4}FeSe$ reported previously
[6]. The magnetic behavior of this superconducting phase,
$(NH_3)_y Na_{0.4}FeSe_{0.5}Te_{0.5}$, has been fully investigated in an
applied magnetic field (H) of 20–40 000 Oe, and the lower
and upper critical fields, H_{c1} and H_{c2}, have been determined.

The β-$FeSe_{1-z}Te_z$ (z = 0 and 0.5) samples (anti-PbO-
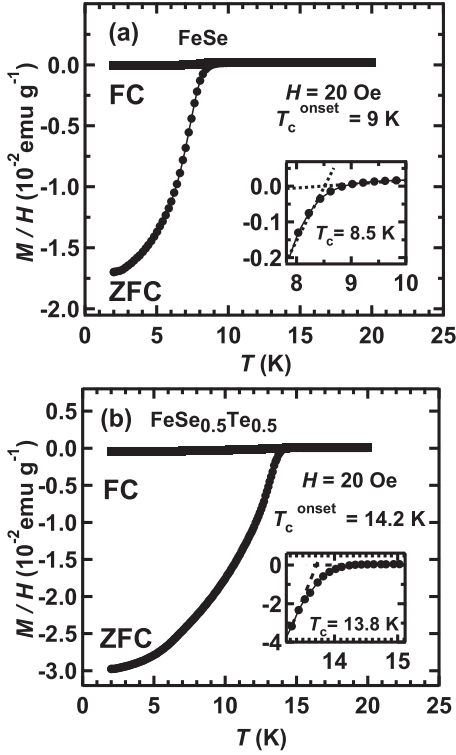type structure) were prepared with the annealing method as

*kubozono@cc.okayama-u.ac.jp

FIG. 1. M/H–T curves of (a) FeSe and (b) FeSe$_{0.5}$Te$_{0.5}$ measured in the ZFC and FC modes. Insets of (a) and (b): the expanded M/H–T curves (ZFC).

described in Refs. [9,10]; the details are described in the Supplemental Material [12]. The dc magnetic susceptibilities, M/H's, of the prepared samples were measured and compared with previous reports [9,10] to ensure sample quality. The M/H was measured with a superconducting quantum interference device (SQUID) magnetometer (Quantum Design MPMS2). The M refers to magnetization. The T_c^{onset} values of the prepared samples [9 K for β-FeSe and 14.2 K for β-FeSe$_{0.5}$Te$_{0.5}$; see Figs. 1(a) and 1(b)] are consistent with those in Refs. [9,10] ($T_c^{onset} = 8$ K for $z = 0$ and $T_c^{onset} = 14$ K for $z = 0.5$ in β-FeSe$_{1-z}$Te$_z$). The shielding fraction was ~100% for both samples at 3 K. For the precise identification of the β-FeSe$_{0.5}$Te$_{0.5}$ sample, the XRD pattern was measured and analyzed using Le Bail fitting with the space group $P4/nmm$ (No. 129). The XRD pattern was measured with wavelength $\lambda = 0.71073$ Å using a Mo $K\alpha$ source (Rigaku R-AXIS RAPID-NR). The lattice constants for the β-FeSe$_{0.5}$Te$_{0.5}$ sample [$a = 3.8420(2)$ Å and $c = 6.0969(3)$ Å] as determined from the XRD pattern are much larger than those of β-FeSe [$a = 3.7747(1)$ Å and $c = 5.5229(1)$] [9], while the a and c were close to those reported previously for β-FeSe$_{0.5}$Te$_{0.5}$ [$a = 3.7909(5)$ Å and $c = 5.957(1)$ Å] [11], establishing that this sample was β-FeSe$_{0.5}$Te$_{0.5}$.

Samples of $(NH_3)_yM_xFeSe_{1-z}Te_z$ (M = Li, Na, and Ca) were synthesized using the liquid NH_3 technique described in Ref. [6]. Experimental details of the synthesis are described in the Supplemental Material [12]. The experimental nominal value, x, of Na is 0.5 in β-FeSe (or $z = 0$) for the low-T_c phase ($T_c^{onset} = 36$ K), and the x is increased to 1.0 in

making high-T_c phase ($T_c^{onset} = 46$ K). The x value is 0.4 for Na and Ca, and 0.5 for Li in β-FeSe$_{0.5}$Te$_{0.5}$ (or $z = 0.5$). Throughout this paper, the chemical composition of samples is represented by the experimental nominal value. The y value, or amount of NH_3, was not determined in this study. The XRD patterns for two phases in $(NH_3)_yNa_xFeSe$ and for $(NH_3)_yNa_{0.4}FeSe_{0.5}Te_{0.5}$ were recorded at 300 K and analyzed using Le Bail fitting with the space group $I4/mmm$ (No. 139). The same x-ray diffractometer (Mo $K\alpha$ source) was used in the XRD measurements.

The M/H curves for the $(NH_3)_yNa_xFeSe$ ($x = 0.5$ and 1.0), $(NH_3)_yNa_{0.4}FeSe_{0.5}Te_{0.5}$, $(NH_3)_yLi_{0.5}FeSe_{0.5}Te_{0.5}$, and $(NH_3)_yCa_{0.4}FeSe_{0.5}Te_{0.5}$ samples were measured using the SQUID magnetometer described above. The M/H curves for the $(NH_3)_yNa_{0.5}FeSe$ and $(NH_3)_yNa_{0.4}FeSe_{0.5}Te_{0.5}$ samples were measured under high pressure with a Be-Cu piston cylinder cell using the same SQUID magnetometer. All samples were introduced into cells (glass capillary for XRD, quartz cell for M/H measurement under ambient pressure, and Be-Cu piston cylinder cell for M/H measurement under high pressure) without any exposure to air in an Ar-filled glove box.

Figure 2(a) shows the M/H curves of $(NH_3)_yNa_{0.5}FeSe$ measured in the zero-field cooling (ZFC) and field cooling (FC) modes as a function of temperature, and the T_c and T_c^{onset} were determined to be 31.5 and 36 K from the M/H curves under ZFC, and $T_c = 32$ K and $T_c^{onset} = 32.5$ K under FC. The determination of T_c is shown in the inset of Fig. 2(a). No superconducting phase of pure β-FeSe was found from the M/H curves in Fig. 2(a). This superconducting phase is distinctly different from that reported previously for $(NH_3)_yNa_{0.5}FeSe$ [3], in which the T_c^{onset} was 46 K. Neither M/H curve in the ZFC nor FC mode indicated the presence of such a high-T_c phase. We made six $(NH_3)_yNa_{0.5}FeSe$ samples. Five samples showed a single T_c^{onset} of ~34 K, while only one sample showed two T_c^{onset}'s (or two superconducting phases) of ~44 and ~36 K. The average T_c ($\langle T_c \rangle$) and the average T_c^{onset} ($\langle T_c^{onset} \rangle$), determined from the M/H curves in the ZFC mode for five samples (low-T_c phase), are 31(2) K and 34(2) K, respectively. Thus, the $(NH_3)_yNa_{0.5}FeSe$ sample prepared with our synthetic method mainly produces the low-T_c phase. The main difference between our synthesis and the previous one [3] is the temperature during synthesis. The former was $-50\,°C$, while the latter was room temperature. Furthermore, we made five $(NH_3)_yLi_{0.5}FeSe$ samples that showed almost the same T_c^{onset} (=42 K) as the previous one, for which $T_c^{onset} = 44$ K [3]. Therefore, it is not clear whether the finding of the low-T_c phase in $(NH_3)_yNa_{0.5}FeSe$ may be due to the low synthesis temperature.

Very recently, we preliminarily tried to vary the nominal x value in making the $(NH_3)_yNa_xFeSe$ samples, and some high-T_c phases (T_c^{onset}~46 K) were successfully prepared in large nominal x value (x~1.0), indicating the different Na amount between low-T_c and high-T_c phases [13]. The XRD patterns of both phases in $(NH_3)_yNa_xFeSe$ samples are shown in Figs. S1 and S2 in the Supplemental Material [12], and the XRD patterns were analyzed with Le Bail fitting to determine the lattice constants. The analyses for both XRD patterns were successfully achieved with the same space group ($I4/mmm$: No. 139), indicating that both phases
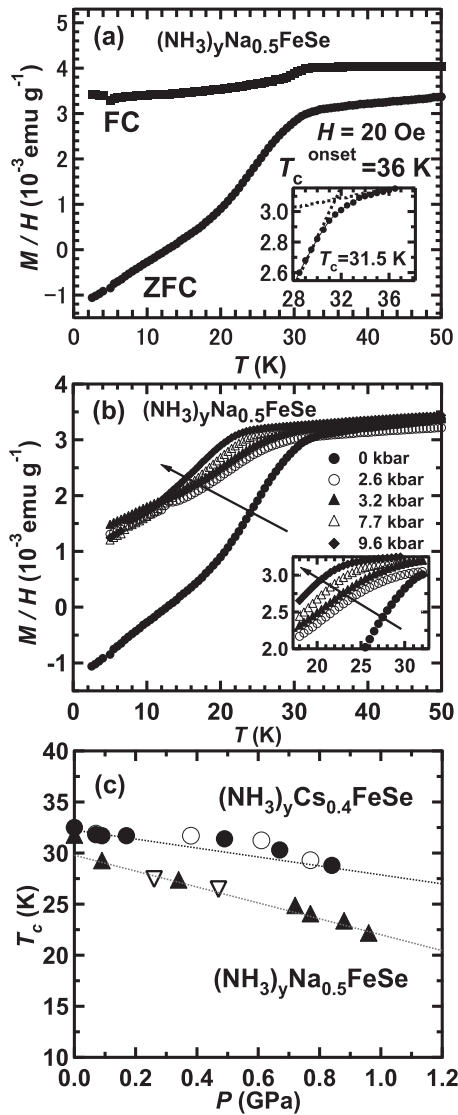
FIG. 2. (a) $M/H–T$ curves of $(NH_3)_yNa_{0.5}FeSe$ measured in the ZFC and FC modes. (b) $M/H–T$ curves of $(NH_3)_yNa_{0.5}FeSe$ measured in the ZFC mode in the pressure range from 0 to 9.6 kbar; 1 GPa = 10 kbar. Insets of (a) and (b): the expanded $M/H–T$ curves (ZFC). (c) $T_c–p$ plots for $(NH_3)_yNa_{0.5}FeSe$ and $(NH_3)_yCs_{0.4}FeSe$. Solid symbols refer to the T_c under increasing pressure, while open symbols refer to the T_c under decreasing pressure.

take the same crystal symmetry. The lattice constants are $a = 3.891(2)$ Å and $c = 14.269(4)$ Å for the low-T_c phase, while they are $a = 3.8275(6)$ Å and $c = 17.579(5)$ Å for the high-T_c phase; the c [17.579(5) Å] of the high-T_c phase is consistent with that [$c = 17.432(1)$ Å] reported previously [3]. The experimental nominal x values in the $(NH_3)_yNa_xFeSe$ samples used for the above XRD measurements were 0.4 for the low-T_c phase and 1.0 for the high-T_c phase. The x value of 0.4 [$(NH_3)_yNa_{0.4}FeSe$] predominantly provided the low-T_c phase ($T_c^{onset} \sim 36$ K) in the same manner as $x = 0.5$ [$(NH_3)_yNa_{0.5}FeSe$]. Here it should be noticed that the x of 1.0 exceeds the feasible x value (=0.5) in the case of the full occupancy of Na at the $2a$ site of the $I4/mmm$ structure, which

means that the experimental nominal value deviates from the real x. We previously determined 0.255(5) as the real x in the $(NH_3)_yCs_{0.4}FeSe$ sample [6], suggesting that the real x value is approximately 50% of the experimental nominal value [6]. To sum up, it can be concluded from the results of XRD that the T_c can be unambiguously scaled by the c, or plane spacing between FeSe layers, as suggested in our previous paper [6]; i.e., the larger c produces the higher T_c. The difference of c in the low-T_c and high-T_c phases may be due to that in the amount of Na (or x). This study is now in progress.

Figure 2(b) shows the M/H curves of $(NH_3)_yNa_{0.5}FeSe$ at different pressures, and the pressure dependence of T_c was determined from the curves. The plot of T_c vs p is shown in Fig. 2(c). The T_c of $(NH_3)_yNa_{0.5}FeSe$ decreases almost linearly with increasing pressure up to 1 GPa, and the T_c's determined while reducing the pressure from 1 GPa are shown on the $T_c–p$ plot made under increasing pressure. The dT_c/dp was determined to be $-7.7(4)$ K GPa^{-1} from the plot in the range from 0 to 1 GPa. In Fig. 2(c), we plotted the T_c of $(NH_3)_yCs_{0.4}FeSe$ as a function of pressure for comparison, based on data from Ref. [6]. The $T_c–p$ plot for $(NH_3)_yCs_{0.4}FeSe$ shows a positive deviation at 0–1 GPa, i.e., the plot deviates positively from a straight line, but the $T_c–p$ plot for $(NH_3)_yNa_{0.5}FeSe$ does not show such a deviation. Consequently, the behavior of T_c in $(NH_3)_yNa_{0.5}FeSe$ shows a simple negative pressure dependence.

We have already investigated the pressure dependence of plane spacing between FeSe layers in $(NH_3)_yCs_{0.4}FeSe$ at 0–40 GPa [14], showing a monotonic decrease with increasing pressure over this wide pressure range. In this pressure range (0–11 GPa) the T_c decreased with increasing pressure despite a small positive deviation at 0–1 GPa [6,14], i.e., the decrease in T_c can be closely related to the decrease in plane spacing. This is exactly consistent with the chemical pressure effect observed for $(NH_3)_yM_xFeSe$ [3,6], in which the T_c becomes lower when the plane spacing is smaller. Although data on the pressure dependence of plane spacing in $(NH_3)_yNa_{0.5}FeSe$ have not yet been reported, the simple negative pressure dependence observed for T_c suggests a simple correlation with plane spacing without any structural phase transition at 0–1 GPa.

Here, we discuss briefly why such a simple negative pressure dependence is observed in the low-T_c phase in $(NH_3)_yNa_{0.5}FeSe$. It is well known that the T_c in FeSe rapidly increases with an increase in pressure up to 4 GPa. The behavior is explained by the scenario that the anion height of FeSe reaches the ideal value (1.39 Å) when applying pressure [10]. Very recently, we investigated the relationship of T_c and anion height in $(NH_3)_yCs_{0.4}FeSe$ based on the pressure dependences of T_c and anion height [14], showing that the T_c decreases regardless of approaching the ideal value of anion height (1.39 Å) by applying pressure. This means that $(NH_3)_yM_xFeSe$ cannot be understood in the analogy with FeSe. Although we cannot clearly answer the origin of difference in pressure dependence between FeSe and $(NH_3)_yM_xFeSe$, the T_c of $(NH_3)_yM_xFeSe$ may decrease owing to the shrinkage of c caused by applying pressure. Actually, the simple shrinkage of c by applying pressure is found in $(NH_3)_yCs_{0.4}FeSe$ [14]. The difference in pressure dependence
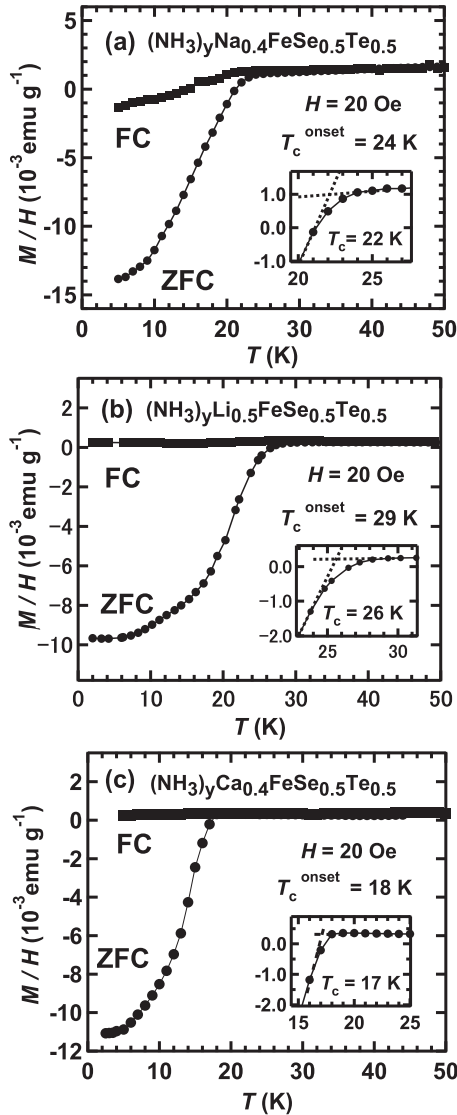
FIG. 3. (a) M/H–T curves of (a) $(NH_3)_y Na_{0.4} FeSe_{0.5} Te_{0.5}$, (b) $(NH_3)_y Li_{0.5} FeSe_{0.5} Te_{0.5}$, and (c) $(NH_3)_y Ca_{0.4} FeSe_{0.5} Te_{0.5}$ as a function of temperature in the ZFC and FC modes. Insets of (a)–(c): the expanded M/H curves (ZFC).

between nondoped and doped FeSe materials is still one of the most important problems to be solved in this research.

Figure 3(a) shows the M/H curves of $(NH_3)_y Na_{0.4} FeSe_{0.5} Te_{0.5}$ measured in the ZFC and FC modes as a function of temperature; the T_c and T_c^{onset} were determined to be 22 and 24 K from the M/H curves in the ZFC mode, respectively, and $T_c = 21$ K and $T_c^{onset} = 23$ K in the FC mode. The shielding fraction of $(NH_3)_y Na_{0.4} FeSe_{0.5} Te_{0.5}$ was evaluated to be 100% at 5 K from the M/H curve in the ZFC mode. In the M/H plots, no superconducting phases of pure β-FeSe and β-FeSe$_{0.5}$Te$_{0.5}$ are observed. We made four $(NH_3)_y Na_{0.4} FeSe_{0.5} Te_{0.5}$ samples, and the $\langle T_c \rangle$ and $\langle T_c^{onset} \rangle$ were determined to be 22(1) K and 23.5(6) K, respectively, from the M/H curves in the ZFC mode for the four samples. The $\langle T_c^{onset} \rangle$ of $(NH_3)_y Na_{0.4} FeSe_{0.5} Te_{0.5}$, at 23.5 K, is lower than the T_c's of $(NH_3)_y Na_{0.5} FeSe$ ($T_c^{onset} = 46$ K in Ref. [3] and $T_c^{onset} = 36$ K in the low-T_c phase found in this study). The

lower T_c^{onset} and T_c observed in $(NH_3)_y Na_{0.4} FeSe_{0.5} Te_{0.5}$ does not support the prediction that a higher T_c may be observed because of the higher T_c (~ 14 K) seen in pure β-FeSe$_{0.5}$Te$_{0.5}$ compared to that (~ 8 K) in pure β-FeSe [9,10]. Furthermore, the observation of higher T_c may be expected because the c of β-FeSe$_{0.5}$Te$_{0.5}$, 5.957(1) Å [11], is larger than that of β-FeSe [5.5229(1) or 5.5234(1) Å] [6,9]. Therefore, it may not be easily explainable that the T_c in $(NH_3)_y Na_{0.4} FeSe_{0.5} Te_{0.5}$ is lower than the T_c's in $(NH_3)_y Na_{0.5} FeSe$.

Furthermore, we measured the XRD pattern of $(NH_3)_y Na_{0.4} FeSe_{0.5} Te_{0.5}$ in order to determine the lattice constants and compare them with those of the high-T_c and low-T_c phases of $(NH_3)_y Na_{0.5} FeSe$. The XRD pattern is shown in Fig. S3 in the Supplemental Material [12]. The Le Bail analysis was performed with the space group ($I4/mmm$, No. 139). The lattice constants are $a = 3.9822(6)$ Å and $c = 17.798(7)$ Å for $(NH_3)_y Na_{0.4} FeSe_{0.5} Te_{0.5}$. Although the c is slightly larger than that [17.578(5) Å] of the high-T_c phase of $(NH_3)_y Na_x FeSe$, the T_c^{onset} (23.5 K) of $(NH_3)_y Na_{0.4} FeSe_{0.5} Te_{0.5}$ is much lower than that ($T_c^{onset} = 46$ K) of the high-T_c phase, indicating that the T_c cannot be universally scaled by c for all metal-doped FeSe$_{1-z}$Te$_z$ materials, i.e., the T_c in $(NH_3)_y Na_{0.4} FeSe_{0.5} Te_{0.5}$ may be universally scaled by the plane spacing of FeSe$_{0.5}$Te$_{0.5}$ layers. To explain the low T_c, we may need to consider additional factors such as structural disorder accompanied by the partial replacement of Se by Te, which may lead to the suppression of a superconducting phase.

Figures 3(b) and 3(c) show the M/H curves of $(NH_3)_y Li_{0.5} FeSe_{0.5} Te_{0.5}$ and $(NH_3)_y Ca_{0.4} FeSe_{0.5} Te_{0.5}$ measured in the ZFC and FC modes as a function of temperature. The T_c and T_c^{onset} for $(NH_3)_y Li_{0.5} FeSe_{0.5} Te_{0.5}$ were, respectively, determined to be 26 and 29 K in the ZFC mode, while $T_c = 26$ K and $T_c^{onset} = 27$ K in the FC mode. The T_c and T_c^{onset} for $(NH_3)_y Ca_{0.4} FeSe_{0.5} Te_{0.5}$ were, respectively, determined to be 17 and 18 K in the ZFC mode, and $T_c = 17$ K and $T_c^{onset} = 18$ K in the FC mode. Consequently, the T_c of Li-doped FeSe$_{0.5}$Te$_{0.5}$ is the highest among Na-, Li-, and Ca-doped samples ($T_c^{onset} = 24$ K for Na, $T_c^{onset} = 29$ K for Li, and $T_c^{onset} = 18$ K for Ca), in contrast to metal-doped FeSe solids, among which Na-doped FeSe is the highest ($T_c^{onset} = 46$ K for Na, $T_c^{onset} = 44$ K for Li, and $T_c^{onset} \sim 40$ K for Ca) [3]. The shielding fractions for $(NH_3)_y Li_{0.5} FeSe_{0.5} Te_{0.5}$ and $(NH_3)_y Ca_{0.4} FeSe_{0.5} Te_{0.5}$ are 80% and 92%, respectively, at 2.5 K. In the M/H curves [Figs. 3(b) and 3(c)], no superconducting phases of β-FeSe$_{0.5}$Te$_{0.5}$ and β-FeSe are found. For $(NH_3)_y Li_{0.5} FeSe_{0.5} Te_{0.5}$, we made only one sample, while for $(NH_3)_y Ca_{0.4} FeSe_{0.5} Te_{0.5}$ four samples were made, and the $\langle T_c \rangle$ and $\langle T_c^{onset} \rangle$ were determined to be 16(1) and 17(1) K, respectively, from the M/H curves in the ZFC mode.

The M/H curves of $(NH_3)_y Na_{0.4} FeSe_{0.5} Te_{0.5}$ at different H are shown in Fig. 4(a). As seen from Fig. 4(a), H was applied from 20 to 40 000 Oe. From the M/H–T curves [Fig. 4(a)], the T_c and T_c^{onset} were determined as a function of H. The H–T_c and H–T_c^{onset} plots are shown in Fig. 4(b). The dashed line was drawn by fitting with an expression, $H = A(T_c - T)^\beta$ for the H–T_c plot. From the dashed line, the H_{c2} was determined to be greater than 40 000 Oe = 4 T at 0 K. The dotted line was drawn by fitting with the same expression for the H–T_c^{onset} plot. From the dotted line, we could evaluate the H_{c2} at 0 K as 17(3) T,
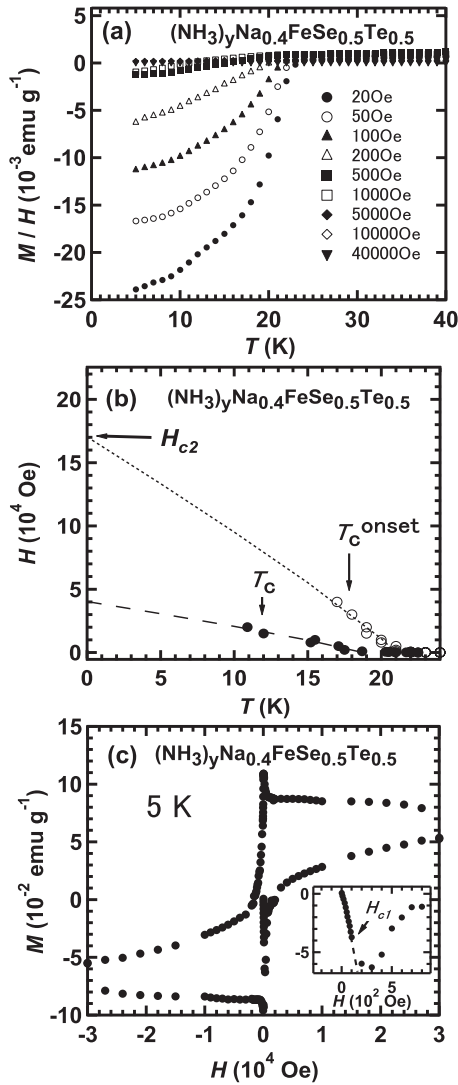
FIG. 4. (a) M/H–T curves of $(NH_3)_y Na_{0.4}FeSe_{0.5}Te_{0.5}$ measured in the ZFC mode in H of 20–40 000 Oe. (b) H–T_c and $H - T_c^{onset}$ plots of $(NH_3)_y Na_{0.4}FeSe_{0.5}Te_{0.5}$ determined from the M/H–T curves shown in (a). (c) M–H curves of $(NH_3)_y Na_{0.4}FeSe_{0.5}Te_{0.5}$ measured at 5 K.

which is close to the H_{c2} of 16.3 T for FeSe polycrsytals [15]. However, the H_{c2} of 17 T is much smaller than the 36.5 T of $(NH_3)_y Ba_{0.4}FeSe$ [3]. The M-H plot measured at 5 K is shown in Fig. 4(c), and the H_{c1} at 5 K was determined to be 100 Oe from the expanded plot [inset of Fig. 4(c)]. In this study, we could not evaluate the H_{c1} at 0 K from the M-T plots [Fig. 4(a)].

The M/H–T plots at different pressures are shown in Fig. 5(a), and the drop in the M/H plot gradually goes to the left as pressure is applied. The pressure dependence of T_c for $(NH_3)_y Na_{0.4}FeSe_{0.5}Te_{0.5}$ is shown in Fig. 5(b). The T_c decreases with increasing pressure. As a reference, in Fig. 5(b) the T_c–p plot of $(NH_3)_y Cs_{0.4}FeSe$ is shown in the graph, as in Fig. 2(c). The T_c–p plots in both phases show a negative pressure dependence, but the fall of the T_c–p plot in $(NH_3)_y Na_{0.4}FeSe_{0.5}Te_{0.5}$ is more rapid than that of $(NH_3)_y Cs_{0.4}FeSe$ [6]. Saturation is

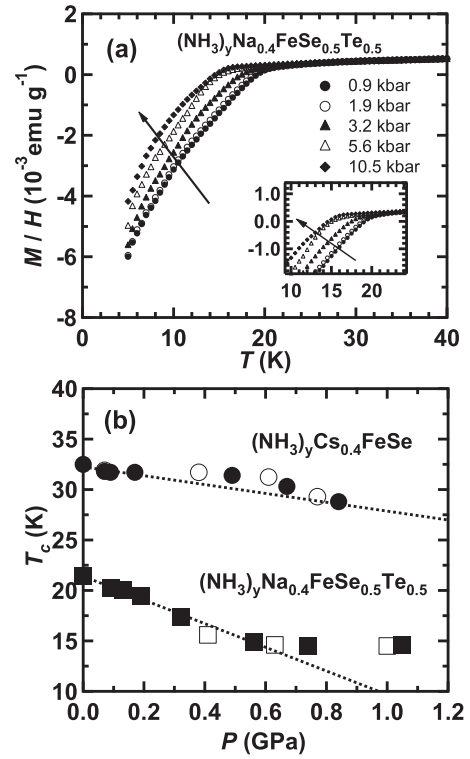FIG. 5. (a) M/H–T curves of $(NH_3)_y Na_{0.4}FeSe_{0.5}Te_{0.5}$ measured in the ZFC mode in the pressure range from 0 to 10.5 kbar: 1 GPa = 10 kbar. Inset: the expanded M/H–T curves (ZFC). (b) T_c–p plots for $(NH_3)_y Na_{0.4}FeSe_{0.5}Te_{0.5}$ and $(NH_3)_y Cs_{0.4}FeSe$. Solid symbols refer to the T_c under increasing pressure, while open symbols refer to the T_c under decreasing pressure.

observed in the T_c–p plot for $(NH_3)_y Na_{0.4}FeSe_{0.5}Te_{0.5}$ above 0.6 GPa, in contrast to $(NH_3)_y Cs_{0.4}FeSe$ [6]. When a linear approximation is applied to the T_c–P plots (0–0.6 GPa) of $(NH_3)_y Na_{0.4}FeSe_{0.5}Te_{0.5}$, the dT_c/dp is approximately $-11.7(5)$ K GPa^{-1} for $(NH_3)_y Na_{0.4}FeSe_{0.5}Te_{0.5}$, while the dT_c/dp is $-4.33(8)$ K GPa^{-1} for $(NH_3)_y Cs_{0.4}FeSe$ [6], and $-7.7(4)$ K GPa^{-1} for $(NH_3)_y Na_{0.5}FeSe$ (in this study). Thus, the dT_c/dp values, $-7.7(4)$ K GPa^{-1} and $-11.7(5)$ K GPa^{-1}, for $(NH_3)_y Na_{0.5}FeSe$ and $(NH_3)_y Na_{0.4}FeSe_{0.5}Te_{0.5}$ are larger than that $[-4.33(8)$ K GPa$^{-1}]$ for $(NH_3)_y Cs_{0.4}FeSe$. Furthermore, it is not clear why saturation is observed in the high-pressure range (0.6 GPa $\leqslant p \leqslant$ 1.0 GPa) of $(NH_3)_y Na_{0.4}FeSe_{0.5}Te_{0.5}$, contrary to $(NH_3)_y Cs_{0.4}FeSe$ and $(NH_3)_y Na_{0.5}FeSe$. The pressure dependence of T_c in $(NH_3)_y Na_{0.4}FeSe_{0.5}Te_{0.5}$ in the pressure range above 1 GPa is of interest to clarify the origin of the saturation, and that work is now in progress.

In conclusion, we have succeeded in multiple syntheses of superconducting phases through the intercalation of alkali and alkali-earth metal atoms into FeSe and FeSe$_{0.5}$Te$_{0.5}$. A superconducting phase was found in $(NH_3)_y Na_{0.5}FeSe$, which is a lower T_c phase than was previously reported [3], indicating the presence of multiple superconducting phases. Furthermore, it has been found that the high-T_c phase possesses a larger c than that of the low-T_c phase in $(NH_3)_y Na_x FeSe$, consistent with the scaling of T_c by c in $(NH_3)_y M_x FeSe$ materials.

The present report details a successful intercalation of metal atoms into $FeSe_{0.5}Te_{0.5}$. The highest T_c found in this study in metal-intercalated $FeSe_{1-z}Te_z$ ($z \neq 0$) is 26 K ($T_c^{onset} = 29$ K) in $(NH_3)_y Li_{0.5} FeSe_{0.5} Te_{0.5}$. The T_c of $(NH_3)_y Na_{0.4} FeSe_{0.5} Te_{0.5}$ is 22 K, which is lower than that of $(NH_3)_y Na_{0.5} FeSe$ ($T_c = 46$ K) [3]. The reason why the T_c of metal-intercalated $FeSe_{0.5}Te_{0.5}$ is lower than that of the corresponding metal-doped FeSe is still unclear. The origin of the effect should be pursued from a structural point of view because the partial replacement of Se by Te may provide structural disorder that suppresses the emergence of the superconducting phase. We found that the T_c cannot be universally scaled by the plane spacing over both metal-intercalated FeSe and $FeSe_{0.5}Te_{0.5}$. The original scaling of T_c by $FeSe_{0.5}Te_{0.5}$ plane spacing may be achieved in metal-doped $FeSe_{0.5}Te_{0.5}$ materials. In this study, we could reproducibly synthesize the same superconducting phases using the same experimental conditions (amount of metal, reaction temperature, reaction time, etc.). Therefore, we could present a complete synthetic protocol for obtaining superconducting phases with $FeSe_{1-z}Te_z$ crystals. The pressure dependence of T_c in the phases found in this study is substantially similar to that in $(NH_3)_y Cs_{0.4} FeSe$ reported previously [6], suggesting the presence of the same physics in $(NH_3)_y M_x FeSe$ and $(NH_3)_y M_x FeSe_{0.5} Te_{0.5}$; the detailed behavior is different and may also provide interesting surprises. This study points the way towards further research in metal-doped $FeSe_{1-z}Te_z$ ($0 \leqslant z \leqslant 1$) because superconducting phases were found and the synthetic protocol was established in this study.

[1] J. G. Guo, S. F. Jin, G. Wang, S. C. Wang, K. X. Zhu, T. T. Zhou, M. He, and X. L. Chen, Phys. Rev. B **82**, 180520(R) (2010).

[2] A. Krzton-Maziopa, Z. Shermadini, E. Pomjakushina, V. Pomjakushin, M. Bendele, A. Amato, R. Khasanov, H. Luetkens, and K. Conder, J. Phys.: Condens. Matter **23**, 052203 (2011).

[3] T. P. Ying, X. L. Chen, G. Wang, S. F. Jin, T. T. Zhou, X. F. Lai, H. Zhang, and W. Y. Wang, Sci. Rep. **2**, 426 (2012).

[4] M. Burrard-Lucas, D. G. Free, S. J. Sedlmaier, J. D. Wright, S. J. Cassidy, Y. Hara, A. J. Corkett, T. Lancaster, P. J. Baker, S. J. Blundell, and S. J. Clarke, Nat. Mater. **12**, 15 (2013).

[5] T. P. Ying, X. L. Chen, G. Wang, S. F. Jin, X. F. Lai, T. T. Zhou, H. Zhang, S. J. Shen, and W. Y. Wang, J. Am. Chem. Soc. **135**, 2951 (2013).

[6] L. Zheng, M. Izumi, Y. Sakai, R. Eguchi, H. Goto, Y. Takabayashi, T. Kambe, T. Onji, S. Araki, T. C. Kobayashi, J. Kim, A. Fujiwara, and Y. Kubozono, Phys. Rev. B **88**, 094521 (2013).

[7] G. J. Ye, J. J. Ying, Y. J. Yan, X. G. Luo, P. Cheng, Z. J. Xiang, A. F. Wang, and X. H. Chen, Phys. Rev. B **86**, 134501 (2012).

[8] T. Takano, T. Kishiume, Y. Taguchi, and Y. Iwasa, Phys. Rev. Lett. **100**, 247005 (2008).

[9] T. M. McQueen, Q. Huang, V. Ksenofontov, C. Felser, Q. Xu, H. Zandbergen, Y. S. Hor, J. Allred, A. J. Williams, D. Qu, J. Checkelsky, N. P. Ong, and R. J. Cava, Phys. Rev. B **79**, 014522 (2009).

[10] Y. Mizuguchi and Y. Takano, J. Phys. Soc. Jpn. **79**, 102001 (2010).

[11] Y. Mizugchi, F. Tomioka, S. Tsuda, T. Yamaguchi, and Y. Takano, J. Phys. Soc. Jpn. **78**, 074712 (2009).

[12] See Supplemental Material at http://link.aps.org/supplemental/10.1103/PhysRevB.89.144509; for details on sample preparation.

[13] L. Zheng, Y. Sakai, M. Izumi, H. Goto, R. Eguchi, L. Sun, J. Kim, A. Fujiwara, and Y. Kubozono (unpublished).

[14] M. Izumi, Y. Sakai, L. Zheng, H. Goto, R. Eguchi, L. Sun, J. Kim, A. Fujiwara, and Y. Kubozono (unpublished).

[15] F.-C. Hsu, J.-Y. Luo, K.-W. Yeh, T.-K. Chen, T.-W. Huang, P. M. Wu, Y.-C. Lee, Y.-L. Huang, Y.-Y. Chu, D.-C. Yan, and M.-K. Wu, Proc. Natl. Acad. Sci. USA **105**, 14262 (2008).